eurasia

RESEARCH ARTICLE

Crystallization Study of Pb Additive Se-Te-Ge Nanostructured Alloys using Non-isothermal Differential Scanning Calorimetry

Balbir Singh Patial[1],*, Neha Sharma[1], Suresh Bhardwaj[2], Nagesh Thakur[1] (iD)

[1]*Department of Physics, Himachal Pradesh University Summerhill, Shimla 171005, India.*
[2]*UGC-DAE Consortium for Scientific Research, University Campus, Khandwa Road, Indore, M.P. -452001, India.*
Corresponding author email: bspatial@hpuniv.ac.in, bspatial@gmail.com

ABSTRACT

Nanotechnology started a new era in research and continuous escalations due to its potential applications. In modern optoelectronics, Pb additive nano-chalcogenides are becoming promising materials. For a memory and switching material, the thermal stability and glass-forming ability are vital, and the glass should be thermally stable from a technological point of view. This research article investigates the thermal behaviour of bulk $(Se_{80}Te_{20})_{94-x}$ Ge_6Pb_x ($x = 0$, 2, 4 and 6) samples under non-isothermal differential scanning calorimetry at four heating rates from 5 to 20°Cmin⁻¹ synthesized using the melt quench procedure. Further, the overall crystallization study, which includes thermal stability, ease of glass formation, fragility, glass relaxation and glass-crystallization transformation kinetics of investigated alloys using different empirical formalisms, is reported and discussed. Compositional and heating rate dependence of recorded characteristic temperatures and other deduced parameters of reheated alloys are also discussed. The correlation between deduced parameters is also established to define the utility of these materials in practical applications.

1. Introduction

Se-Te system is better as it has higher photosensitivity, greater hardness, higher crystallization temperature and more ageing effects as compared to pure amorphous selenium. Further doping of the third element in the Se-Te system creates configurational and compositional disorder [1]. Also, chalcogenide glasses with the parent Se-Te system were accomplished acceptance due to distinctive features such as reversibility and optical nonlinearity. An earlier study from our lab indicates that doping of Ge to Se-Te system increases the degree of cross-linking, glass transition temperature, and crystallization

temperature and enhances its thermal stability [2], motivating us to consider $(Se_{80}Te_{20})_{94}Ge_6$ as the base sample to synthesize quaternary alloys. Metallic dopants such as Pb significantly alter the electronic and thermal properties of chalcogenide alloys [3, 4]. Pb is the primary material of modern infrared optoelectronics. When Pb is added to the Se-Te-Ge system, it enhances the conductivity and the reason for the transition from *p* to *n*- type. Pb is a heavy atom, making the system denser. In our previous study on dielectric and *AC* conductivity measurements in Se-Te-Pb shows the significant impact on its conduction mechanism with the addition of Pb and it is observed that $Se_{79}Te_{20}Pb_1$ is a critical composition at which maxima occurs

and the system becomes a chemically ordered alloy containing comparatively higher energy hetero-polar bonds [4].

Lead (Pb) additive chalcogenide materials are basic materials of contemporary IR optoelectronics, and being the heaviest atom, it provides compactness to thus prepared compound materials. Moreover, interest is towards quaternary alloys for opto-electronic applications. In this decade, Pb-additive chalcogenide alloys have been widely explored for the technological implications in IR detectors and emitters, photo-resistors, lasers and solar devices. Chalcogenide nano range alloys have size-dependent properties. Because of this, they show spectacular variations in their properties like thermo-physical, optical, electrical etc [5-7]. Though Pb is toxic but enhances the properties of these materials and leads to synthesis of these materials in nano-range. Our lab executed the melt quenching experiment for $(Se_{80}Te_{20})_{94-x}Ge_6Pb_x$ with $0 \leq x \leq 12$ again [8]. It is observed in the x-ray diffraction pattern that higher Pb content leads to more intense peaks indicating that thermal history during melt quenching experiment has a profound impact on the synthesis of these materials in the nano-range [6, 8]. Further, in other melt quenching experiments from our lab, bulk samples of similar composition i.e. $(Se_{80}Te_{20})_{94-x}Ge_6Bi_x$ with $0 \leq x \leq 12$, were synthesized by replacing Pb with Bi to explore the properties with the addition of Bi and to circumvent Pb being toxic [9]. It is observed that Bi is also acted as a modifier in the synthesis of nano-crystalline Bi additive Se-Te-Ge samples.

The thermal stability of melt quenched alloys is determined more precisely and also for examining nucleation-growth aspects that happen due to the transition of the metastable phases in the glassy alloy. At the same time, it is reheated in differential scanning calorimetry (DSC) or differential thermal analysis (DTA) experiment. The present research paper reports the data about the thermal studies of $(Se_{80}Te_{20})_{94-x}Ge_6Pb_x$ ($0 \leq x \leq 6$) alloys at four heating rates from 5 to 20°C/min using non-isothermal differential scanning calorimetry technique and overall non-isothermal crystallization kinetics were reported and discussed.

2. Experimental details

Bulk samples of $(Se_{80}Te_{20})_{94-x}Ge_6Pb_x$ ($0 \leq x \leq 6$) were synthesized using the procedure mentioned

elsewhere [10]. Structural characterizations, x-ray diffraction and FESEM confirmed the nano nature of investigated Pb additive quaternary alloys [11]. The thermal behaviour is studied using non-isothermal DSC by using the Mettle Toledo star DSC system with similar specific parameters given in other research paper [11]. The temperature accuracy of this equipment is ±0.1°C in the measured values. Approximately, 3-5 mg of sample in powder form is encapsulated in the standard aluminium pan in an atmosphere of dry nitrogen at a heat flow of 40 mL min^{-1} and heated at different heating rates from 5 – 20°Cmin^{-1}. Thermograms so obtained may be separated into three regions; endothermic peaks (glass transition and melting), whereas exothermic peaks correspond to crystallization. Correspondingly, characteristic temperatures T_g (glass transition), T_o (onset crystallization), T_p (crystallization) and T_m (melting) are also recorded. In observations and calculations, peak values of T_g, T_p and T_m are taken instead of onset values because of more accuracy in measuring peak values than onset values. The least-squares fitting technique is applied to deduce apparent activation energies and other kinetic parameters while using empirical approaches.
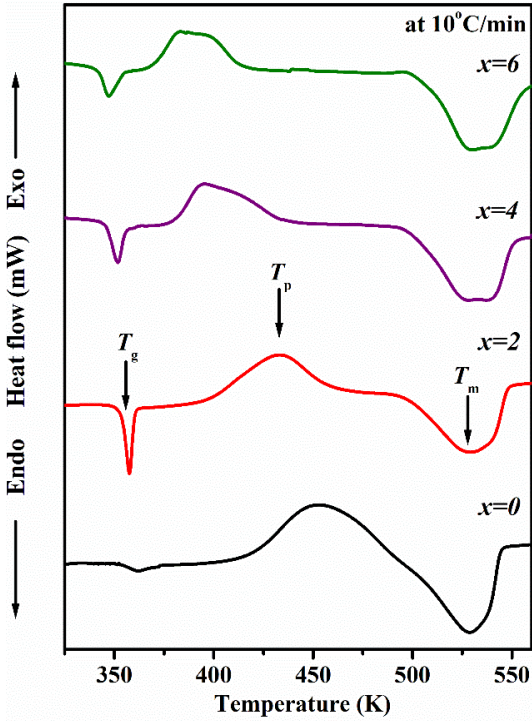
3. Results and discussion

Figure 1 shows traces for $(Se_{80}Te_{20})_{94-x}Ge_6Pb_x$ ($0 \leq x \leq 6$) at a heating rate of 10°C per minute and figure 2 shows traces for $(Se_{80}Te_{20})_{92}Ge_6Pb_2$ at four heating rates from 5 – 20°Cmin^{-1}. Similar thermograms were also observed for other investigated alloys, and at other heating rates (not shown here) and well defined endothermic and exothermic peaks were found.

3.1 Heating Rate Dependence of Characteristic Temperatures

All examined samples show single T_g and single T_p indicating that the investigated system exists in a single phase and is homogeneous. It is observed that characteristic temperatures shift to higher temperatures with increasing heating rates (α). At T_g, structural relaxation time becomes equal to the relaxation time of observation τ_{ob} [12]. Since $T_g \propto 1/\tau_{ob}$. Thus, the increase in a, τ_{ob} decreases leads to increased T_g also observed in other glasses [13]. It can also be ascribed that heat dissipated so much easier at a higher heating rate; therefore, decomposition begins at a relatively higher

temperature and has a higher heat of fusion. T_p is also found to increase (similar to T_g) with an increasing heating rate. This could be because the materials do not get enough time for nucleation and crystallization with a higher heating rate.

3.2 Thermal Stability and GFA

The thermal stability of a glassy material is an essential factor from a technological point of view in various applications. It has been ascertained based on calorimetric observations. Kauzmann proposed a two-third rule to determine the ease in glass formation [14] by a parameter called reduced glass transition temperature T_{rg} ($=T_g/T_m$). $T_{rg} \sim 2/3$ for all investigated alloys is signifying good glass-forming ability (GFA) (Table 1).

Hruby number K_{gl} is another important parameter by which thermal stability and glass formation is

Figure 1. DSC thermograms of $(Se_{80}Te_{20})_{94-x}$ Ge_6Pb_x (x = 0, 2, 4 and 6) at 10°C/min.
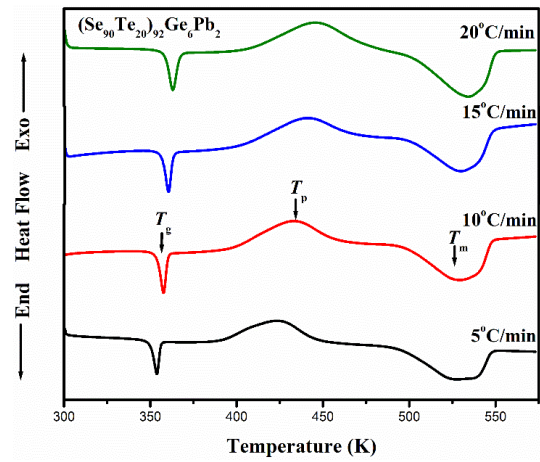
Figure 2. DSC thermograms of $(Se_{80}Te_{20})_{92}Ge_6$ Pb_2 at four heating rates (5, 10, 15 and 20°C/min).

Sample	Thermal parameters	Heating rates			
		5°C/min	10°C/min	15°C/min	20°C/min
$(Se_{80}Te_{20})_{94}Ge_6$	T_{rg}	0.68	0.69	0.69	0.69
	K_{gl}	0.96	1.18	1.27	1.47
	Fi	31.24	21.63	18.23	16.33
$(Se_{80}Te_{20})_{92}Ge_6Pb_2$	T_{rg}	0.67	0.68	0.68	0.68
	K_{gl}	0.67	0.79	0.91	0.95
	Fi	33.44	23.13	19.52	17.51
$(Se_{80}Te_{20})_{90}Ge_6Pb_4$	T_{rg}	0.66	0.67	0.67	0.67
	K_{gl}	0.29	0.32	0.35	0.37
	Fi	35.61	24.59	20.76	18.68
$(Se_{80}Te_{20})_{88}Ge_6Pb_6$	T_{rg}	0.65	0.66	0.66	0.66
	K_{gl}	0.22	0.24	0.26	0.27
	Fi	37.16	25.67	21.67	19.52

Table 1. Reduced glass transition temperature (T_{rg}), Hruby number (K_{gl}) and fragility index (F_i) determined from the heating rate data for $(Se_{80}Te_{20})_{94-x}Ge_6Pb_x$ (x = 0, 2, 4 and 6).

evaluated as $(T_p - T_g)/(T_m - T_p)$ [15]. Glass transition temperature also gives useful information about the thermal stability related to strength and rigidity of glass structure. GFA is also associated with cooling of the melt, bypassing crystallization. It has been stated that $(T_p - T_g)$ is also an indicator of GFA. The higher the value of this difference, the greater is GFA. Higher $(T_p - T_g)$ delays nucleation while lower $(T_m - T_p)$ retards growth in nucleated crystals. Thus, Hruby's parameter merges nucleation and growth information during amorphous-crystallization phase transformation. For $K_{gl} \leq 0.1$, a good glass-forming ability has not been obtained [12]. The deduced values are found to decrease with increasing Pb content (Table 1), but these values are well above the limit indicating good GFA of examined alloys.

3.3 Glass Transition Region

First endothermic region in reheating experiment is known as the glass transition region. Glass transition temperature depends upon the coordination number, bond energy and types of structural units formed. It can be studied as a variation of T_g with heating rate and apparent activation energy. T_g denotes the strength of the glass structure. In this paper, three empirical methods are used to study the dependence of T_g on a and to estimate apparent activation energy. First approach is Lasocka's relation; $T_g = A + B\ln(a)$ [16]. Here A and B are constants. A indicates T_g at a heating rate of 1K per minute and can be obtained from the intercept of the straight-line plot between $\ln(\alpha)$ and T_g. Similarly, B can be obtained from the slope and is related to the cooling rate of melt. The physical significance of B could be related to the structural changes within the glass transition region. This empirical expression holds very well for all examined samples (figure 3), and derived values of A and B are given in table 2.

The apparent activation energy of thermal relaxation can be understood by glass transition kinetics. The other approach is the estimation of apparent activation energy for the glass transition E_g from the dependence of T_g on a using Kissinger's relation [17] and Moynihan et al. relation [18]. Kissinger's equation is extensively used to deduce the activation energy of crystallization. This relation could be used to estimate the E_g as the curve or variation is similar to estimate the Eg as the curve or variation is similar to the crystallization process. The plot using this relation for $(Se_{80}Te_{20})_{92}Ge_6Pb_2$ is shown in figure 4, and deduced values of E_g are given in table 2 for all investigated samples. There is an increase in E_g with increasing Pb content and reverse order compared to the constant B.

Similarly, in the other approach, i.e. using Moynihan's relation, linear fit variation of $\ln(\alpha)$ against $1000/T_g$ for $(Se_{80}Te_{20})_{92}Ge_6Pb_2$ is shown in figure 4. Other samples are also offering similar variations (not shown here). Deduced E_g values for
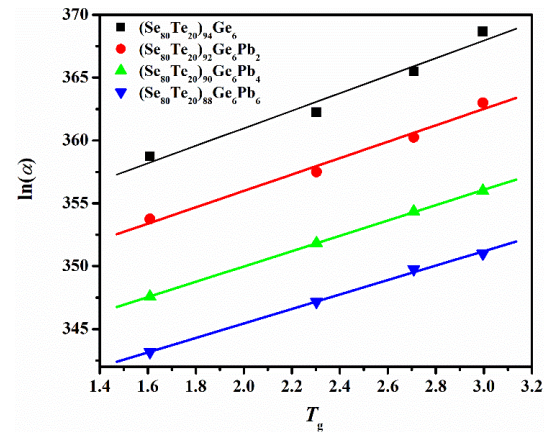
Figure 3. ln (α) versus T_g plots for $(Se_{80}Te_{20})_{94-x}$ Ge_6Pb_x (x = 0, 2, 4 and 6).

Sample	A	B	E_g(kJ/mol)	
			Kissinger's equation	Moynihan et al approximation
$(Se_{80}Te_{20})_{94}Ge_6$	347.02	6.97	146.96	153.01
$(Se_{80}Te_{20})_{92}Ge_6Pb_2$	342.94	6.52	155.30	161.34
$(Se_{80}Te_{20})_{90}Ge_6Pb_4$	337.69	6.15	162.71	168.55
$(Se_{80}Te_{20})_{88}Ge_6Pb_6$	333.23	6.11	167.74	173.51

Table 2. Constants A(K), B(min) and activation energy of the glass transition region E_g for $(Se_{80}Te_{20})_{94-x}$ Ge_6Pb_x (x = 0, 2, 4 and 6) samples.

all samples under investigation are given in table 2 and are found in concordance with Kissinger's relation; therefore, one can use either of these two approaches. Moreover, E_g is found to increase with higher doping of Pb by both the approaches and trends are in reverse concerning B (cooling rate of melt) concludes thermal transformations with Pb content.

There are no standard criteria for parameterising glass formation. For measuring GFA of the glassy system, the fragility index (F_i) is a significant parameter. F_i signifies the rate through which relaxation time reduces with temperature around T_g. It is calculated through the relationship mentioned elsewhere [19] by taking the average of the glass transition activation energy of the two methods (Table 2). It is stated by Viglis [20] that glass-forming liquids that reveal approximate dependence on Arrhenius temperature are characterized as solid good glass forming liquids. These liquids have a low value of F_i ($F_i \approx 16$), whereas the high value of F_i ($F_i \approx 200$) signifies the limit of fragile glass-forming liquid [19]. At the

Figure 4. Variation of $\ln(\alpha/T_g^2)$ and $\ln(\alpha)$ against $1000/T_g$ for $(Se_{80}Te_{20})_{92}Ge_6Pb_2$.
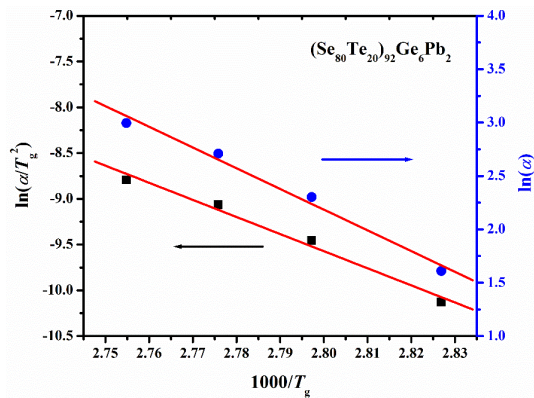
same time, fragile glass-forming liquids show non-Arrhenius behavior. For examined composition at four heating rates, F_i is calculated and is listed in table 1. As calculated F_i values are within the above-mentioned limit, it is reasonable to state that investigated chalcogenide systems are primed from strong glass the above-mentioned limit.

3.4 Crystallization region

Further reheating after structural relaxation results in crystallization. Crystallization process is linked with nucleation and growth phenomena. Usually, different activation energies must be marked to nucleation and growth phenomena during the amorphous-crystallization transition. But, as a whole, total apparent activation energy is taken into consideration, combining both aspects representing the overall crystallization phenomenon. Crystallization region is studied based on several theoretical models. The apparent crystallization activation energy E_c is achieved via heating rate dependence of crystallization temperature. The first one is Kissinger's relation, and aparent E_c is deduced as done earlier for T_g in subsection 3.3, and its values for all examined samples are listed in table 3. Further, in another approach, Mahadevan *et al.* [21] have estimated E_c by replacing $\ln(a/T_p^2)$ with $\ln(a)$ in Kissinger's relation (Table 3). Figure 5 shows a variation to evaluated E_c using these different methods for $(Se_{80}Te_{20})_{94}Ge_6$. Similar plots are also observed for other examined samples (not shown here). The third method used to derive apparent E_c is called Augis and Bennett method [22], as given below:

$$ln\left[\frac{\alpha}{T_p - T_o}\right] = -\frac{E_c}{RT_p} + lnk_o \qquad (1)$$

The slope of the graph plotted between $\ln(a/(T_p - T_o))$ against $1/T_p$ will provide E_c (Table 3).

Sample	Kissinger's Formula	Mahadevan approximation	Augis and Bennett approximation	Augis and Bennett Method	
	E_c(kJ/mol)	E_c(kJ/mol)	E_c(kJ/mol)	E_c(kJ/mol)	k_o (s^{-1})
$(Se_{80}Te_{20})_{94}Ge_6$	89.34	96.71	93.10	72.88	1.27×10^9
$(Se_{80}Te_{20})_{92}Ge_6Pb_2$	89.50	96.87	93.12	78.56	1.28×10^{10}
$(Se_{80}Te_{20})_{90}Ge_6Pb_4$	106.16	112.75	109.46	80.60	4.69×10^{11}
$(Se_{80}Te_{20})_{88}Ge_6Pb_6$	123.62	129.98	126.81	86.18	6.63×10^{12}

Table 3. The activation energy for crystallization E_c deduced from different methods and k_o(s^{-1}) for $(Se_{80}Te_{20})_{94-x}Ge_6Pb_x$ ($x = 0, 2, 4$ and 6) samples.
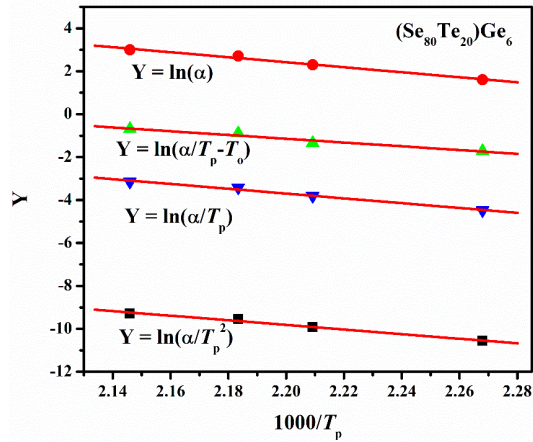
Figure 5. Plot of Y ($Y = \ln(\alpha/T_p^2)$, $\ln(\alpha)$, $\ln(\alpha/(T_p-T_o))$ and $\ln(\alpha/T_p)$) versus $1000/T_p$ for $(Se_{80}Te_{20})_{94}Ge_6$.

The application of the Augis and Bennett method involves accurate assessment of T_o which is dependent on precision during DSC curve fitting. In addition, the origin ordinate gives the frequency factor (k_o), which increases with increasing Pb content. This indicates the lesser crystallization tendency in glasses containing a higher concentration of Pb. The values of k_o for all investigated samples are given in Table 3. In the case of $T_p > T_o$, equation (1) can be approximated and may be called as Augis and Bennett approximation, in which left-hand side is replaced by $\ln(a/T_p)$, and E_c can be estimated [23] (Figure 5 and Table 3).

The activation energies for crystallization are calculated using different formulas that differ substantially from each other (Table 3). A considerable difference for the same material may result from taking different approximations for the final outcome of these approaches. Kissinger's relation is the standard method used for analyzing the crystallization process in transformation for first-order reaction. Augis and Bennett method (equation (1)) is also beneficial as k_o can be deduced along with apparent E_c.

3.5 Compositional dependence of T_g and T_p

Variation of peak temperature of glass transition with Pb doping amount for $(Se_{80}Te_{20})_{94-x}Ge_6Pb_x$ ($0 \leq x \leq 6$) at four heating rates (5–20ºC/min) is shown in figure 6. The reduction in T_g with increasing Pb content may be due to structural
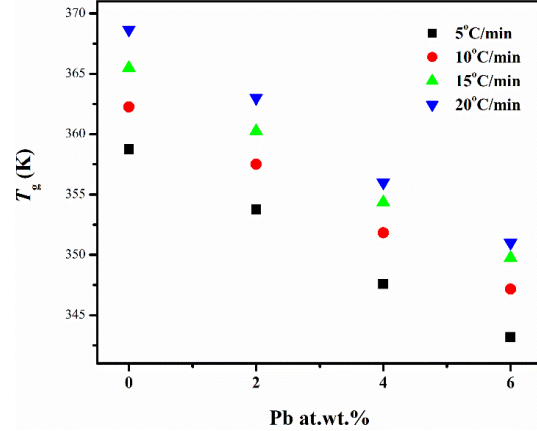
Figure 6. Variation of T_g with Pb at.wt.%.
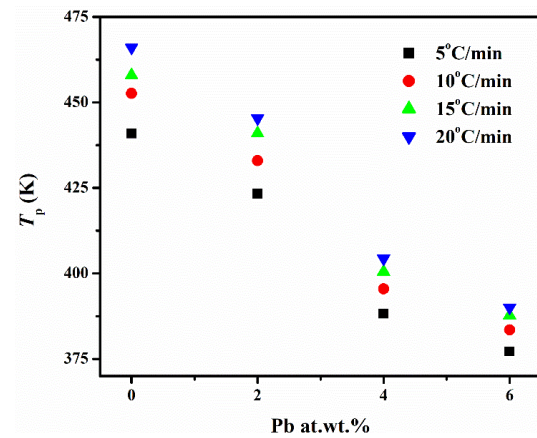
Figure 7. Variation of T_p with Pb at.wt.%.

changes that occurred with Pb addition. Se has about 40% ring structure, with 60% being confined as polymeric chains. Doping of Pb in Se-Te based rich system favours bond formation with Se and Te separately and reduces the adequate bond energy. Therefore, T_g decreases. Figure 7 shows the variation of T_p with Pb at.wt.% for investigated composition, and a similar trend as T_g is also observed. In addition, it can also be seen that with increasing Pb concentration, there is an increase in T_g with heating and is different for each sample and especially 15 and 20 degrees Celsius per minute, the difference in T_g is very minute. It can also be attributed to higher heat dissipation at a higher heating rate.

The apparent glass transition activation energy increases with Pb content, i.e. a reverse trend is found in comparison to T_g. A similar trend is also observed for the apparent activation energy for crystallization region as compared to T_p. Hruby

number is also showing decrement with the increase in Pb at.wt.% at all heating rates. Lesser T_g above room temperature may tend to self transition and hence declines the practical utility of the sample.

4. Conclusions

Overall Crystallization kinetics was made on bulk samples of $(Se_{80}Te_{20})_{94-x}Ge_6Pb_x$ ($0{\leq}x{\leq}6$) synthesized by melt quenching procedure using DSC under non-isothermal conditions. Characteristic temperatures viz glass transition and crystallization temperatures are observed to increase with the increase in heating rate. But these temperatures are showing decreasing trend on higher Pb doping. Using different empirical approaches, the apparent activation energy is calculated for the endothermic (glass transition) and exothermic (crystallization) process. The concordance in apparent glass transition activation energy using Kissinger's method and Moynihan *et al* relation deduce that one can use either of two equations. But the considerable difference in deduced values of apparent activation energy for crystallization by different empirical approaches indicates the impact of various approximations taken while deriving the final equation. Two-third rule is observed in all investigated samples. The deduced Hruby number values and fragility index are indicating good GFA of examined alloys.

Acknowledgements

References

[1]   Patial BS, Thakur N, Tripathi SK. On the crystallization kinetics of In additive Se–Te chalcogenide glasses. Thermochim. Acta. 2011; 513:1-8. doi: 10.1016/j.tca.2010.09.009

[2]   Mainika, Bhatt SS, Thakur N. Calorimetric studies and thermal stability of $(Se_{80}Te_{20})_{100-x}Ge_x$ (x = 0, 2, 4 and 6) chalcogenide glasses by thermal analysis. J. Optoelectronics and Advanced Materials. 2009; 11:1860-1864.

[3]   Vashist P, Patial BS, Anjali, Tripathi SK, Thakur N. Iso-conversional study of crystallization activation energy of amorphous-crystallization transformation for $Se_{79}Te_{20}Pb_1$ glass using non-isothermal differential scanning calorimetry technique, Indian J. Pure Appl. Phys. 58 (2020) 135–140. http://nopr.niscair.res.in/handle/123456789/54217

[4]   Thakur A, Patial BS, Thakur N. On the Dielectric Study of $Se_{80-x}Te_{20}Pb_x$ (x = 0, 1 and 2) Glasses. J. Electron. Mater. 2017; 46 (3):1516-24. DOI: 10.1007/s11664-016-5190-1

[5]   Mourdikoudis S, Pallares RM, Thanh TKN. Characterization techniques for nanoparticles: comparison and complementarity upon studying nanoparticle properties. Nanoscale. 2018; 10:12871-934. DOI: 10.1039/C8NR02278J

[6]   Kooi BJ, Wuttig M. Chalcogenides by Design: Functionality through Metavalent Bonding and Confinement. Advanced Materials. 2020; 32(21): 1908302. DOI: 10.1002/adma.201908302

[7]   Deepika, Dixit M, Singh H, Attia MS, Amin MA. Recent innovations in properties of nanostructured glasses and composites. J. Exp. Nanoscience. 2021; 16 (1): 180-211. DOI: 10.1080/17458080.2021.1940221

[8]   Vashist P, Patial BS, Bhardwaj S, Awasthi AM, Tripathi SK, Thakur N. Structural transition and thermophysical study of quaternary $(Se_{80}Te_{20})_{94-x}Ge_6Pb_x$ ($0{\leq}x{\leq}12$) alloys. Phase Transitions. 2022; 95(4): 308-321. https://doi.org/10.1080/01411594.2022.2042537

[9]   Vashist P, Patial BS, Thakur N. Synthesis and investigation of topological behaviour and structural modification in Se-Te-Ge-Bi nanostructured alloys. Applied Surface Science Advances. 2022; 8:100220. https://doi.org/10.1016/j.apsadv.2022.100220

[10] Sharma N, Patial BS, Thakur N. Dielectric Study of Chalcogenide $(Se_{80}Te_{20})_{94}Ge_6$ Glass. AIP Conf. Proc. 2018; 1942: 070008. doi: 10.1063/1.5028806

[11] Sharma N, Patial BS, Thakur N. Structural analysis and theoretical investigations in Pb additive Se-Te-Ge chalcogenide nano-composites. *Ind. J. Pure & Appl. Phys.* 2018; 56: 128 – 135. http://op.niscair.res.in/index.php/IJPAP/article/view/17881

[12] Anjali, Patial BS, Bhardwaj S, Awasthi AM, Thakur N. On the crystallization kinetics of multicomponent nanochalcogenide

Se$_{79-x}$Te$_{15}$In$_6$Pb$_x$ (x=0, 1, 2, 4, 6, 8 and 10) alloys. Nano Express. 2020; 1: 030021. https://doi.org/10.1088/2632-959X/abc8c7

[13] Zheng Q, Zhang Y, Montazerian M, Gulbiten O, Mauro JC, Zanotto ED, Yue Y. Understanding Glass through Differential Scanning Calorimetry. *Chem. Rev.* 2019; 119(13): 7848–39. https://doi.org/10.1021/acs.chemrev.8b00510

[14] Kauzmann W. The Nature of the Glassy State and the Behavior of Liquids at Low Temperatures. *Chem. Rev.* 1948; 43: 219-256. https://doi.org/10.1021/cr60135a002

[15] Hruby A, Czech. *J. Phys. B***22** (1972) 1187.

[16] Lasocka M. The effect of scanning rate on glass transition temperature of splat-cooled Te$_{85}$Ge$_{15}$. Mater. Sci. Eng. 1976; 23 (2-3): 173-177. https://doi.org/10.1016/0025-5416(76)90189-0

[17] Kissinger HE. Variation of Peak Temperature With Heating Rate In Differential Thermal Analysis. *J. Res. Nat. Bur. Stand.* 1956; **57 (4)**: 217-21. https://nvlpubs.nist.gov/nistpubs/jres/057/jresv57n4p217_a1b

[18] Moynihan CT, Easteal AJ, Wilder J, Tucker J, Dependence of the Glass Transition Temperature on Heating and Cooling Rate.

J. Phys. Chem.1974; **78 (26)**: 2673-77. https://doi.org/10.1021/j100619a008

[19] Tripathi SK, Patial BS, Thakur, N. Glass transition and crystallization study of chalcogenide Se$_{70}$Te$_{15}$In$_{15}$ glass. J. Therm. Anal. Calorim. 2012; 107:31-38. https://doi.org/10.1007/s10973-011-1724-1

[20] Viglis TA. Strong and fragile glasses: a powerful classification and its consequences. Phys Rev B. 1993; 47:2882–2885. https://doi.org/10.1103/PhysRevB.47.2882

[21] Mahadevan S, Giridhar A, Singh AK. Calorimetric measurements on as-sb-se glasses. J. Non-Cryst. Solids. 1986; 88 (1): 11. https://doi.org/10.1016/S0022-3093(86)80084-9

[22] Augis JA, Bennett JE, Calculation of the Avrami parameters for heterogeneous solid state reactions using a modification of the Kissinger method. J. Therm. Anal. 1978; 13: 283. https://doi.org/10.1007/BF01912301

[23] Yinnon H, Uhlmann DR. Applications of thermoanalytical techniques to the study of crystallization kinetics in glass-forming liquids, part I: Theory. J. Non-Cryst. Solids. 1983; 54(3) 253-75. https://doi.org/10.1016/0022-3093(83)90069-8